Structure of ultrathin SiO_2/Si(111) interfaces studied by photoelectron spectroscopy

J. W. Keister[a] and J. E. Rowe[b),c)]
Department of Physics, North Carolina State University, Raleigh, North Carolina 27695-8202

J. J. Kolodziej
Department of Physics and Astronomy and Laboratory for Surface Modification, Rutgers University, Piscataway, New Jersey 08855-0849

H. Niimi
Department of Materials Science and Engineering, North Carolina State University, Raleigh, North Carolina 27695-8202

H.-S. Tao and T. E. Madey
Department of Physics and Astronomy and Laboratory for Surface Modification, Rutgers University, Piscataway, New Jersey 08855-0849

G. Lucovsky
Department of Physics, North Carolina State University, Raleigh, North Carolina 27695-8202

(Received 25 February 1999; accepted 3 May 1999)

Device-grade ultrathin (9–22 Å) films of silicon dioxide, prepared from crystalline silicon by remote-plasma oxidation, are studied by soft x-ray photoelectron spectroscopy (SXPS). The $2p$ core-level spectra for silicon show evidence of five distinct states of Si, attributable to the five oxidation states of silicon between Si^0 (the Si substrate) and Si^{4+} (the thin SiO_2 film). The relative binding energy shifts for peaks Si^{1+} through Si^{4+} (with respect to Si^0) are in agreement with earlier work. The relatively weaker signals found for the three intermediate states (I_1, I_2, and I_3) are attributed to silicon atoms at the abrupt interface between the thin SiO_2 film and substrate. Estimates of the interface state density from these interface signals agree with the values reported earlier of ~ 2 monolayers (ML). The position and intensity of the five peaks are measured as a function of post-growth annealing temperature, crystal orientation, and exposure to He/N_2 plasma. We find that annealing produces more abrupt interfaces (by reducing the suboxide interface state density), but never more abrupt than ~ 1.5 monolayers. We observe a 15%–20% drop in the interface thickness (in particular the ''Si^{2+}'' peak intensity) with increasing annealing temperature. Somewhat different behavior is observed with small amounts of nitrogen in the SiO_2 film where an apparent increase in interface state density is seen. A quantitative analysis is presented which explores the effects of these sample preparation parameters in terms of relative interface state density and modeling of the SXPS data. © *1999 American Vacuum Society.* [S0734-2101(99)22704-2]

I. INTRODUCTION

In the present study, we use high-resolution soft x-ray photoelectron spectroscopy (SXPS) with synchrotron radiation and Auger electron spectroscopy (AES) to study ultrathin SiO_2 gate oxides grown on Si(111) that achieve device-quality interface conditions. A crucial issue that continues to inhibit understanding of spectroscopic SiO_2/Si measurements is sample preparation at the device-grade level of processing such that interface details can be usefully compared to electrical measurements. We decided to reinvestigate the issue of the interface of SiO_2/Si(111) using the current state-of-the-art methods of gate oxide growth. The detailed atomic structure and number of interface states for ultrathin-oxide interfaces of SiO_2/Si ($\sim 10-40$ Å) remains a somewhat controversial topic with some arguing for atomically abrupt (i.e., ~ 1 monolayer, ML) interfaces while others propose a larger transition region of ~ 10 Å thickness.[1–6] Previous SXPS measurements by Himpsel *et al.*[2] gave an interface width of 3–5 Å (~ 2 ML) for both (111) and (100) interfaces. Our results show an interface that is about 30% smaller probably related to improved sample growth. Standard interface capacitance and other electrical measurements done on the same wafer as our electron spectroscopic experiments characterized the samples as device grade.[7–11]

The bulk Si($2p$) binding energy for Si(111) is ~ 99.3 eV and the bulk Si($2p$) oxide value for film thickness $\geqslant 30$ Å SiO_2 is ~ 103.7 eV.[1] The binding energies of the three interface-shifted peaks are intermediate between these values and have been assigned by Himpsel *et al.*[2] as suboxide states of Si atoms usually labeled Si^{1+}, Si^{2+}, and Si^{3+} with the bulk Si peak labeled Si^0 and the bulk oxide peak labeled

[a)]Also at: National Research Council Postdoctoral Associate at the Army Research Office.
[b)]Physics Division, Army Research Office, Research Triangle Park, NC 27709-2211; electronic mail: jrowe@aro-emhl.army.mil
[c)]Also at: Department of Physics and Astronomy and Laboratory for Surface Modification, Rutgers University, Piscataway, NJ 08855-0849.

Si^{4+}.[2–5] *Because the formal oxidation state interpretation has recently been called into question, we prefer to use a notation of* I_1, I_2, *and* I_3 *rather than* Si^{1+}, Si^{2+}, *and* Si^{3+} *for the interface peaks*.[3–5] The relative intensity of each specific interface Si peak is known to depend on oxide/interface quality, and intensities can be varied by changing the surface sensitivity. For example, the wafer surface orientation [Si(111) vs Si(100)] determines the interface intensity ratios seen in SXPS. In addition, changing the surface sensitivity provides a crude means of depth profiling of the various suboxide states.[2] Another known effect is the strong dependence of the SiO_2 peak binding energy on SiO_2 film thickness on the range 5–100 Å.[1] Unfortunately, binding energy values for various previous studies are not entirely consistent for the same film thickness (perhaps due to differences in oxide quality). Thus, we have reinvestigated the Si($2p$) peak binding energy dependence on SiO_2 film thickness for each of the five peaks with SXPS in the present study.

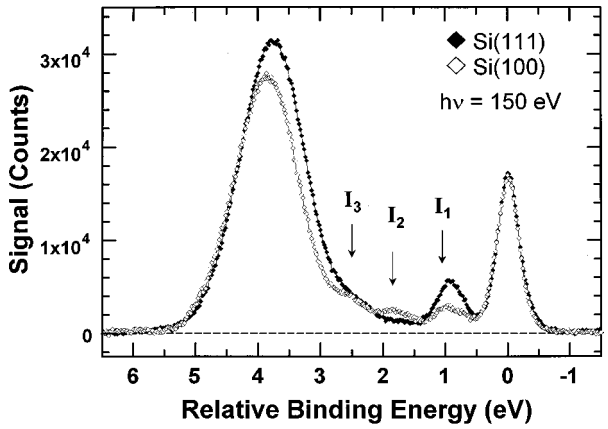

FIG. 1. SXPS Si($2p$) data for a film of ~10 Å thickness, grown on Si(111) and measured at a photon energy of 150 eV. The lower $2p_{1/2}$ spin-orbit component was stripped and the background subtracted. For comparison, similar data for Si(100) are overlayed. Both samples were annealed by RTA at 900 °C.

II. EXPERIMENTAL DETAILS

A. Growth of SiO_2 films

The ultrathin SiO_2 samples were made using plasma-enhanced oxidation. First, native oxide layers on Si(111) substrates were removed by etching in 40% NH_4F for 4 min and then rinsing for 1 min with de-ionized water. These steps produced H-terminated Si(111) surfaces which was heated in vacuum to 300 °C and exposed to excited oxygen species extracted from a remote He/O_2 radio frequency (rf) plasma. The He and O_2 were flowed at 200 and 20 $cm^3\,min^{-1}$, respectively, at a total chamber pressure of 0.3 Torr, with the 13.56 MHz rf plasma power fixed at 30 W. On-line (i.e., *in situ*) AES measurements characterized the growth rate, which followed a power law SiO_2-film thickness dependence, $t_{ox} \approx 7t^{0.28}$, where t_{ox} is the SiO_2 thickness in Å and t is plasma exposure time in minutes.[9] The SiO_2 films reported in this study (measured by SXPS to be in the range 9–22 Å) were made using exposure times of approximately 5 s to nearly 10 min.

Nitridation of the SiO_2–Si interface was achieved by further exposing the plasma-oxidized Si(111) wafer to active nitrogen species from a remote rf He/N_2 plasma for 45–120 s with He and N_2 flows of 160 and 60 $cm^3\,min^{-1}$, respectively. During this process, N atoms preferentially migrate to the Si–SiO_2 interface, where they are localized at the interface, forming Si–N bonds.[12–14] Single oxidized wafers were broken *ex situ* and one fragment is annealed at a temperature in the range, $T = 700$–900 °C by rapid thermal annealing (RTA) in Ar, providing a means of comparing of ''as-grown'' and annealed samples under the same oxidation conditions.

B. SXPS measurements

After growth and annealing, the samples were exposed to air at atmospheric pressure over 1–5 days prior to being transferred to the SXPS apparatus. After pumping to ultra-high vacuum ($\sim 1\times10^{-10}$ Torr) with a three-chamber load-lock system, the samples were annealed in vacuum to ~500 °C to remove weakly bound atmospheric-pressure induced adsorbates. The SXPS configuration at the U4A beamline of the National Synchrotron Light Source (NSLS) includes a 6 m toroidal grating monochromator (TGM) which produces a photon beam with ≤0.1 eV resolution at photon energies ($h\nu$) of 10–200 eV.[15,16] The photon energies in the range 130–170 eV have this ~0.1 eV resolution, but the fixed exit slit configuration offers only ~0.15 eV resolution at 200 eV. The photoelectron kinetic energy (KE_e) was measured with a VSW 100 mm hemispherical analyzer fixed at 45° to the photon beam axis. Most spectra were obtained with the sample surface facing the analyzer at the normal emission geometry ($\alpha = 90°$ take-off angle). Although some data were collected at $\alpha \approx 40°$ from the surface plane and the electron analyzer was used in fixed pass energy mode with a resolution of ~0.1 eV.

The reference Fermi energy (E_F) was measured using a metal sample attached to the same sample holder. The E_F threshold appeared at a kinetic energy of 4.6 eV less than the photon energy, and the Si(111) substrate ($2p_{3/2}$) peak appeared at a binding energy ($h\nu - E_F - KE_e$) of 99.4 eV. This small deviation from the standard value of 99.3 eV can possibly be attributed to some residual charging with apparent bias (~0.1 eV) of the sample. However, this shift does not affect the binding energy of the oxidized states measured relative to the Si substrate peak position (for SiO_2 films of thickness less than ~50 Å).[1] The sample SiO_2 film thickness was estimated from the Si($2p$) SXPS spectra using the electron escape depth values reported as a function of energy by Himpsel *et al.*[2]

III. EXPERIMENTAL RESULTS

A. Comparison of Si(111) and Si(100) substrate orientations

Typical Si($2p$) core-level stripped raw data (with the inelastic electron background subtracted) are shown in Fig. 1

for both Si(111) and Si(100) substrates for thin SiO_2 films. As is usually the custom for Si($2p$) SXPS data, we applied a simple spin-orbit stripping procedure[2–6] to remove the S($2p_{1/2}$) component leaving the stripped raw data for the Si($2p_{3/2}$) component. Evidence of three interface bonding states is clearly seen as three weak peaks (I_1, I_2, and I_3) with binding energies intermediate between the Si($2p$) peaks of the bulk Si substrate and SiO_2 film. Detailed discussion of the Si(100) data will be done in another publication, but it is clear that the interface peak intensity is strongly dependent on Si substrate crystal orientation. These differences are qualitatively similar to those reported by Himpsel *et al.*[2] as well as others.[3–6] The samples used for these measurements are ~10 Å thick and have been annealed at 900 °C. Similar data and orientation dependence have been found for SiO_2 film thickness in the range 9–22 Å.

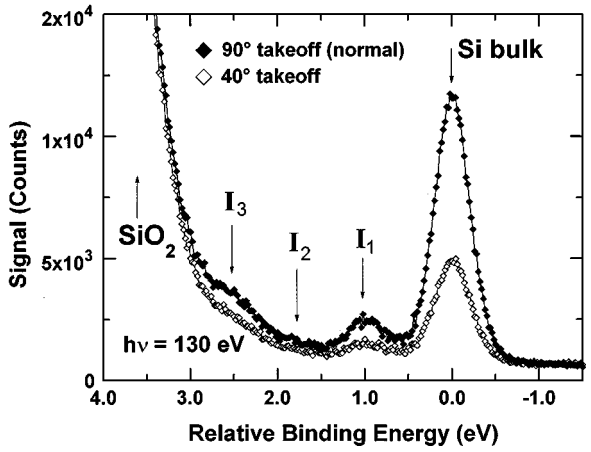

FIG. 2. Angle-resolved SXPS data taken for the same sample at two different takeoff angles (40° and 90°). The two data sets are normalized using the $SiO_2(2p)$ peak height. The reduction in Si substrate and interface peaks shows that the suboxide signal comes from the interface.

B. Angular dependence and surface effects

In order to verify that the interface states reside at the Si–SiO_2 interface (and not at the SiO_2 film top surface), we measured some samples at different takeoff angles. This procedure is known to be effective for quantitatively determining surface components at high kinetic energies (~1000 eV or greater) but is problematic at lower kinetic energies typical of the present experiments (~100 eV) for crystalline surfaces, due to photoelectron diffraction effects. Fortunately, the present samples have amorphous SiO_2 surface regions and diffraction effects are minimal; thus diffraction can be neglected. [For comparison to Si(100), see the recent report of Si(100)–SiO_2 interface ordering in Ref. 17.] The angle tilting experiment changes the nominal SiO_2 film thickness t_{ox} to an ''effective'' thickness t_{eff} by the relation:

$$t_{\text{eff}}=\frac{t_{\text{ox}}}{\sin\alpha}, \tag{1}$$

where α is defined as the angle between the analyzer and the surface plane ($\alpha=90°$ is normal; small angles are glancing). Figure 2 shows angle-resolved SXPS data taken for the same sample at two different takeoff angles ($\alpha=40°$ and $\alpha=90°$). The two data sets are normalized to the same SiO_2 peak height, which effectively takes into account the difference in illuminated area with tilt angle.[6,17] The reduction in suboxide and Si substrate peaks shows that the suboxide signal comes from the interface and not from the surface. A comparison of the photon energy dependence of the suboxide state intensities further reveals that the I_1 state lies closest to the Si substrate (in this case, SiO_2 film thickness is constant but escape depth changes). Earlier data for Si(111) reported by Himpsel and co-workers gave evidence of the I_3 component being distributed over a range of thicknesses throughout the SiO_2 film, but their samples were grown by different methods and could have different interface properties. In fact, the I_3 peak intensities reported by Himpsel are about 40% higher than in the present study.

We can quantitatively estimate the fraction of suboxide density, which occurs near the top surface of the SiO_2 film based on such data. First, we write the total two-dimensional suboxide state density N_{tot} as a sum of density at the interface (N_{int}) and surface (N_{top}) locations:

$$N_{\text{tot}}=N_{\text{top}}+N_{\text{int}}, \tag{2}$$

and define the surface fraction R by:

$$R=\frac{N_{\text{top}}}{N_{\text{top}}+N_{\text{int}}}. \tag{3}$$

Thus, the Si substrate-normalized suboxide signal, I_j/I_0, can be calculated from

$$\frac{I_j}{I_0}=\frac{N_{\text{tot}}[R+(1-R)e^{-t_{\text{eff}}(\alpha)/\lambda_{\text{SiO}_2}}]}{\left(\frac{\sigma_{\text{Si}}}{\sigma j}\right)n_{\text{Si}}\lambda_{\text{Si}}e^{-t_{\text{eff}}(\alpha)/\lambda_{\text{SiO}_2}}}, \tag{4}$$

where n_{Si} is the three-dimensional density of bulk Si substrate, λ_{Si} and λ_{SiO_2} are the energy-dependent electron escape depths in Si and SiO_2, respectively, and $\sigma_{\text{Si}}/\sigma_j$ is the photoemission cross-section ratio for the suboxide state j relative to Si. Using the angle-resolved data shown in Fig. 2, we have determined that these suboxide species occur principally (~95%) at the interface. The parameters R and N_{tot} roughly correspond to slope and intercept of the normalized intensity curve as a function of takeoff angle (although with two points, the fit is exact). The results of this type of analysis for the three suboxide states (I_1, I_2, and I_3) of Fig. 2 are given in Table I.

TABLE I. Angle-resolved experimental results.

j	$I_j/I_0(40°)$	$I_j/I_0(90°)$	N_{tot}	R
1	0.171	0.149	$4.1_5\times10^{14}$ cm^{-2}	0.055
2	0.072	0.044	1.0×10^{14} cm^{-2}	0.035
3	0.360	0.243	4.6×10^{14} cm^{-2}	0.023

C. SiO_2 film-thickness dependent binding energy

In addition to the expected SiO_2 to Si-substrate intensity-ratio dependence with film thickness, we found a monotonic thickness dependence for the binding energy shift. This result is consistent with a well-known[18–20] core-hole screening effect in which the SiO_2 final state ($2p^+$ core-hole) potential is screened by image charges resulting from the dielectric discontinuity at the interface with Si and at the top surface of the SiO_2 film. In thin SiO_2 films, electrons ejected from the Si atoms in the SiO_2 layer have a reduced binding energy due to the coulomb interaction with the core hole (positive ion) because they also feel the repulsion (screening) of its image charge in the Si substrate. There is an additional contribution due to the SiO_2 film-vacuum interface which is comparatively weak and becomes important only for SiO_2 films thicker than about 20 Å. For thinner samples, the dominant effect of increasing SiO_2 thickness is to increase the separation between the photoelectrons formed near the surface and the dielectric image charge, thus increasing the relative binding energy (ΔBE). This trend is shown in Fig. 3(a).

That the binding energy shift with film thickness is predominantly a screening effect can be readily shown by comparison with the magnitude of the image-charge correction calculated as in Refs. 19 and 20. The relevant equation is

$$\Delta BE(z,d)=\frac{e}{4\pi\epsilon_0 k_2}\sum_{n=0}^{\infty}(ab)^2\left[\frac{a}{n2d+2z}+\frac{b}{(n+1)2d-2z}+\frac{2ab}{(n+1)2d}\right], \tag{5}$$

where d is the SiO_2 film thickness, z is the distance from the Si substrate ($0<z<d$), e is the elemental charge, ϵ_0 is the permittivity of free space, and k_1, k_2, and k_3 are the dielectric constants of the silicon substrate, SiO_2 film, and vacuum, respectively. The values a and b are given by

$$a=\frac{k_1-k_2}{k_1+k_2}, \tag{6a}$$

and

$$b=\frac{k_2-k_3}{k_2+k_3}. \tag{6b}$$

The binding energy shift δBE which results from this screening effect is an additive correction to the ''zero-order'' shift ΔBE_0, which becomes a parameter in the data fitting. Therefore, the total shift for SiO_2 relative to Si (ΔBE) is given by

$$\Delta BE=\Delta BE_0+\delta BE. \tag{7}$$

The value δBE which we use is obtained as the electron-escape-depth-weighted screening potential, averaged over the SiO_2 film thickness, neglecting the unphysical boundary conditions of the model which occur within 1.6 Å of the SiO_2 film edges, as discussed in Ref. 20. We find that averaging the peak positions in this way is equivalent to finding the peak position of a weighted sum of Gaussian peak shapes. Dielectric constants for Si and SiO_2 of 11.8 and 2.1,[21] respectively, are used with an electron escape depth in the SiO_2 film $\lambda(SiO_2)=4.8$ Å at a photon energy of 150 eV (electron kinetic energy of ~50 eV). We find a fit to our data with a ΔBE_0 value of 4.17 eV (103.5 eV binding energy) which agrees with previously published values.[1,2] For SiO_2 films ranging in thickness between 9 and 20 Å, the slope of the $\Delta BE/t_{ox}$ curve is ~ 0.03 eV Å^{-1}.

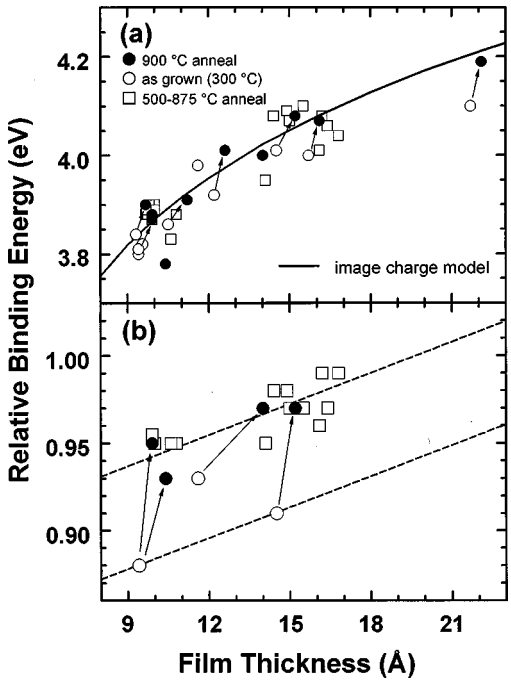

FIG. 3. Binding energy shift of (a) SiO_2 film and (b) I_1 interface states with SiO_2 film thickness. In addition to the gradual slope of ~0.03 eV/Å for the SiO_2 film peak in the annealed samples (shown as solid symbols), there is a ~65 meV shift observed upon annealing for both of the states shown. Arrows indicate samples which are derived from the same wafer (same oxidation treatment) and differ only in that the open symbols represent wafer segments which were not further annealed and solid symbols represent the segments from the same wafer which were annealed *ex situ* to 900 °C by RTA in Ar.

Thus, we have measured the film thickness dependence of the SiO_2 binding energy and it matches the screening effect calculation. The plot of ΔBE vs t_{ox} in Fig. 3 also helps to distinguish film thickness effects from treatment effects such as post-oxidation annealing temperature. Shown in Fig. 3(b) is the same type of ΔBE vs t_{ox} data for the I_1 peak. Although this interface state does not show the same strong ΔBE shift effect with SiO_2 film thickness as does the SiO_2 peak (presumably because its location is fixed at the interface regardless of t_{ox}), it does show quite dramatically an annealing effect which both states share. SXPS data for the 900 °C annealed and the ''as-grown'' wafer segments show dramatically different ΔBE's for the I_1 and SiO_2 film states, as represented in Fig. 3 by arrows pointing from the ''as-grown'' data to the 900 °C anneal data from the same wafer. A 0.065 eV shift is experienced by both states which indicates a conversion of suboxide states to SiO_2 near the interface and throughout the SiO_2 film, as we discuss in the following section.

TABLE II. Typical fitting parameters used (present data and * Ref. 2).

j	ΔBE (eV)	FWHM (eV)
0	-0-	~0.36
1	0.96	0.44*
2	1.84*	0.58*
3	2.5*	0.66*
4	~4	~1.15

IV. INTERFACE STATE ANALYSIS

A. Fitting procedure

Our purpose in this work is primarily to identify trends in interface state densities as a function of post-growth annealing. In a preliminary fitting step, we measured the relative binding energies and found values which were in agreement with previous work.[2] Subsequent fits were performed with the three interface state peak widths and two of the three positions held fixed using the previously determined values. By including such constraints, we can obtain higher precision for the interface state intensities. In addition, this has allowed us to clearly track the positions of the I_1 (interface) and SiO_2 (film) peaks with film thickness and annealing treatment.

Although the data shown in this article have had the inelastic electron background and $(2p_{1/2})$ spin-orbit component removed for clarity, we have obtained spectral parameters by fitting the raw data with a model function which includes the background and spin-orbit components. The $(2p_{1/2})$ spin-orbit component was taken as signal at a fixed 0.602 eV splitting and statistical 1:2 ratio. The best fits were obtained using a nonlinear least-squares procedure that has been previously described.[22,23] Peaks were fit with Voigt functions with ~0.1 eV Lorentzian full width at half maximum (FWHM), and variable Gaussian widths which were kept fixed during fitting at values taken from Ref. 2 for the suboxide peaks, but was freely varied for the SiO_2 film and Si substrate components which dominate the spectra. In all cases, the total width of the Voigt profiles used was dominated by the Gaussian component, which represents a quadrature sum of the instrumental width ($\leqslant$0.15 eV), the phonon broadening, and any inhomogeneous disorder broadening. Typical fitting parameters used are given in Table II.

B. Annealing effects in thin SiO_2 films

Typical fitted data are shown in Fig. 4. The fitting functions are used to quantify the annealing effect, which is predominantly a reduction of the I_2 signal for these Si(111) samples. Fitting parameters obtained from many samples were used to identify trends. In particular, the effect of post-oxidation annealing was explored. Since the absolute interface peak intensities depend on SiO_2 film thickness, we normalized the individual interface-state peak area by the Si substrate peak area in order to allow comparison of the large group of samples with various SiO_2 film thicknesses. Quantitative measurement of (two-dimensional) interface electronic state densities from our SXPS data are possible using

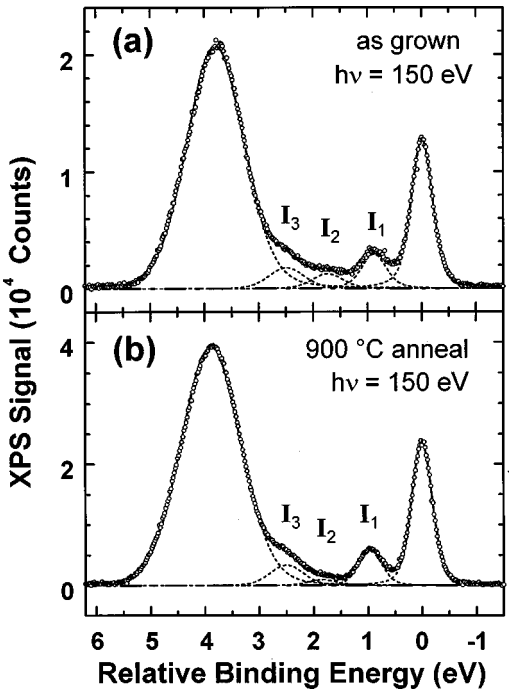

FIG. 4. Spin-orbit stripped and background subtracted Si$(2p)$ data, fit with five Voigt profiles using the reference parameters listed in Table II. Panel (a) shows data for an ''as-grown'' sample (~12 Å), and panel (b) is for a fragment of the same wafer, annealed *ex situ* to 900 °C by RTA in Ar.

previously estimated values for electron escape depths and relative photoemission cross sections for the five oxidation states observed. These estimates, based on Ref. 2, allow us to extract individual and total interface state densities, by the following equation:

$$\Theta_j = \frac{I_j}{I_0} \cdot \frac{\sigma_{\mathrm{Si}}}{\sigma_j} \cdot \frac{n_{\mathrm{Si}} \cdot \lambda_{\mathrm{Si}}}{N_{(111)}}, \tag{8}$$

where Θ is the coverage (in Si substrate monolayers), I_j/I_0 is the Si substrate-normalized peak intensity, $\sigma_{\mathrm{Si}}/\sigma_j$ is the ratio of state photoemission cross sections including the atom density ratio [derived from Ref. 2 and our data (and listed in Table III)]. The parameter n_{Si} is the three-dimensional Si crystal density, λ_{Si} is the electron escape depth, and $N_{(111)}$ is the two-dimensional density of Si atoms on the (111) surface of crystalline Si (a single monolayer). Thus, the average I_j/I_0 ratios are calculated for a range of annealing temperatures, and the individual interface bonding state densities are calculated according to Eq. (8). The results for O_2-only oxidations are shown in Fig. 5.

The I_1 and I_3 interface states appear to be intrinsic to the Si(111)–SiO_2 interface and therefore remain constant despite

TABLE III. Coverage measurement parameters (present data and * Ref. 2).

$h\nu$ (eV)	λ_{Si} (Å)	$\sigma_{\mathrm{Si}}/\sigma_1$	$\sigma_{\mathrm{Si}}/\sigma_2$	$\sigma_{\mathrm{Si}}/\sigma_3$
130	3.3*	1.0*	0.91*	0.59*
150	4.8	1.0	1.0	0.68
200	6.3	1.0	1.0	0.77

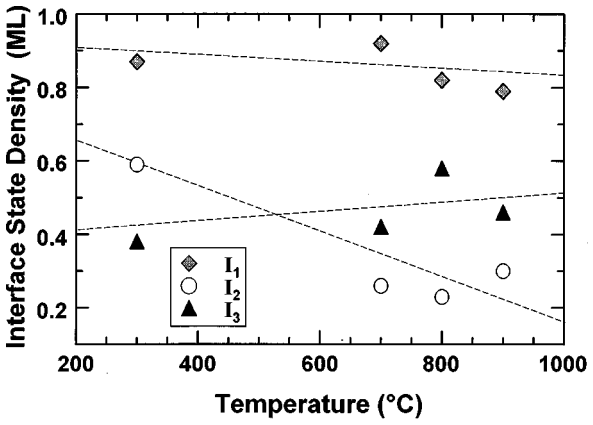

FIG. 5. Interface bonding state densities for the states I_1, I_2, and I_3 found in the SXPS spectra, for O_2-only oxidation. The ~1 ML of Si^{1+} is expected to be an intrinsic feature of the SiO_2/Si(111) interface arising from the single bonds available at the Si substrate. Similarly, Si^{3+} is expected for this interface for 1 ML offsets in the interface position which might arise from minimal interface roughening. Thus, these interface state densities remain constant during annealing. The I_2 peak however, is not an intrinsic feature and is effectively reduced (~60%) by annealing. 300 °C is the oxidation temperature (this is the ''as-grown'' sample). Dashed lines are drawn to illustrate the trends.

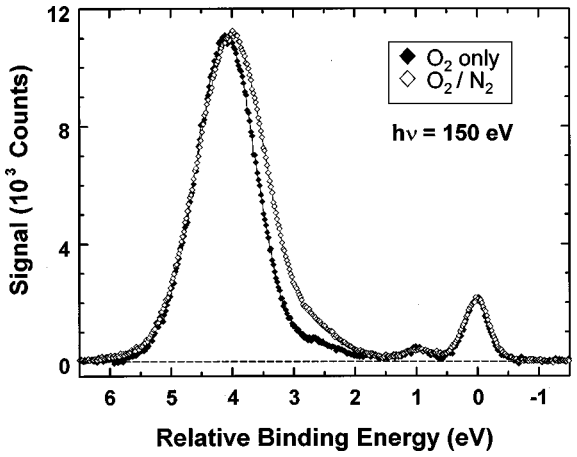

FIG. 6. Spectral comparison of samples with and without nitrogen incorporated at the SiO_2/Si interface. Both data sets are for ~15.3 Å total oxide thickness. Peak width and interface signal both increase with N incorporation.

annealing. The I_2 peak, however, is not an intrinsic feature, and thus is effectively reduced (~60%) by annealing, as shown in Fig. 5. The total interface density for Si(111), $\Theta_{tot}=(\Theta_1+\Theta_2+\Theta_3)$, thus drops 20% from 1.84 monolayers (ML) ($1.44\times10^{15}\,cm^{-2}$) to 1.56 ML ($1.22\times10^{15}\,cm^{-2}$) between 300 and 900 °C as a result of reduction of the excess interface state which we might interpret as Si^{2+}. This final density is 13% lower than reported in Ref. 2. In addition to the ΔBE shift resulting from SiO_2 film thickness (image charge effect), the annealing effect of ~65 meV is also a clue to interface structure. This effect can be explained in terms of second-neighbor effects or slight geometric changes (bond lengths and angles) which result from relaxation of the system to a lower-energy state during annealing. Our data are consistent with the SiO_2 film becoming more crystalline, giving the surface more charge and pulling interface Si atoms toward the SiO_2 film. A simple geometric shift which explains the ΔBE shift (for the Si^{1+} state in contact with the Si substrate) is interface Si atoms moving into the SiO_2 film, shortening Si–O interaction lengths and lengthening Si–Si distances. In this way, the initial and final state effects work in the same direction: to increase the measured binding energy. The initial state energy is lowered due to increased polarization (charge transfer from Si) of the Si–O bond, to lower its energy and make it more ionic. The final state effect (screening of the core hole by image charge) is decreased when the interface Si atoms increase their distance from the Si substrate, also resulting in increased binding energy.

C. Nitrided interface results and discussion

The effect of incorporation of nitrogen at the Si(111)–SiO_2 interface was also explored using the N_2 plasma exposure technique. In Fig. 6 are shown spectra for Si(111) oxidized with and with without 90 s N_2^* exposure, annealed at 900 °C, where N_2^* is the (unknown) excited N species in the plasma. Normally the nitridation produces films which are somewhat thicker overall. Thus, we are comparing samples which have slightly different oxidation conditions in order to compare films of equal total film thickness. The main effect of nitrogen incorporation at the interface on the SXPS data is to increase the peak widths and interface signal strength. Thus, the material is clearly more complex, with more variety of chemical environments available to Si atoms. Unfortunately, the nitride components cannot be distinguished easily from the oxide states. So, we have analyzed these data with the same five peak model as for the oxide films: five Voigt-function profiles which correspond loosely to the (oxygen) oxidation states of Si. The resulting fits for such interface data seem more mixed than for the pure oxide. That is, the I_1 state does not dominate the interface as much, and the I_3 state appears more important. However, an important limitation to the interpretation of these data is the fact that the Si($2p$) chemical shift due to N atoms is only ~70% of that for O atoms. Therefore, we are neglecting contributions from possible SiN_xO_y states which do not have peaks near the same positions as in the SiO_2/Si system. For example, the N_3SiO environment of silicon oxynitride (Si_2N_2O) has an expected ΔBE of 3.1 eV which is nearly midway between Si_2O_3 (Si^{3+}, at 2.5 eV) and SiO_2 (Si^{4+}, at ~4 eV). Similarly, we may be counting N-rich regions (i.e., the first suboxide monolayer) as an unrelated suboxide state. (For example, Si_3N_4 has roughly the same binding energy as the Si_2O_3 ''Si^{3+}'' state in the SiO_2/Si system.) We plan to investigate further the characteristics of thin SiN_xO_y materials in order to clarify some of these results in the future. However, we are justified in the present analysis for the following three reasons: (i) most of the signal comes from the surface where the nitrogen atom number density is low, (ii) the N atom percent in the film is less than 20%, and (iii) mixed oxynitride states of Si are well modeled by the

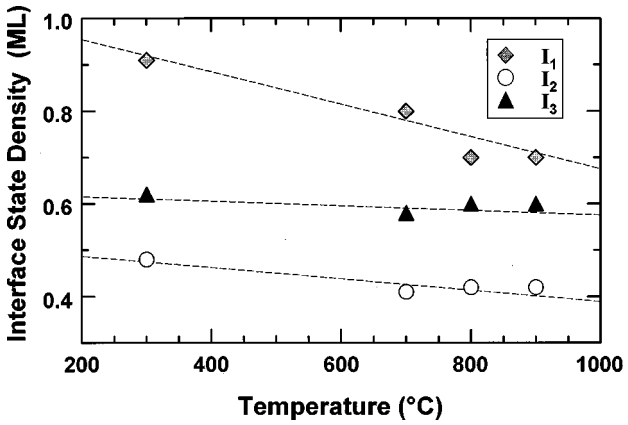

FIG. 7. Individual interface state densities for SiO_2 films with nitrogen incorporation at the Si(111)–SiO_2 interface. Annealing identifies the interface excess as predominantly the I_1 state. The I_2 state density is lower to begin with than for the pure oxide, whereas the I_3 state density is higher. 300 °C is the oxidation temperature (this is the ''as-grown'' sample). Dashed lines are drawn to illustrate the trends.

same Voigt profiles, only with larger widths (FWHM) and perhaps lower ΔBE. In fact, the chemical shift for the SiO_2 film (Si^{4+}) peak is lower than that for the pure oxide by ~ 0.2 eV. This may result from a reduced oxidation state of Si due to some N incorporation in the film, or it may be due to reduced effective film thickness (image charge effect) due to interface N atoms behaving electrically as an extension of the Si substrate. Figure 7 shows the average individual interface state densities for these samples with nitrogen incorporation at the interface, as a function of post-oxidation annealing temperature.

For comparison, Fig. 8 shows the total interface state density, $\Theta_{tot}=(\Theta_1+\Theta_2+\Theta_3)$, for the pure oxide and nitrided interface samples. Both types of samples show considerable suboxide reduction upon annealing. The increased interface density of the nitrided-interface sample may be due to the ~ 1 ML of N coverage in addition to a (perhaps reduced) oxygen-only suboxide region. Since the silicon nitride to silicon oxide relative photoemission cross sections are not known, we have assumed they are all unity. Doing so, we find that the nitrided interface density is $\sim 10\%$ greater than that for the pure SiO_2 samples. The total interface density reduces $\sim 15\%$ (compared to $\sim 20\%$ for pure oxide) upon annealing at 900 °C. The final interface density is $1.35 \times 10^{15}\,cm^{-2}$. The reduction due to annealing is predominantly due to removal of excess ''Si^{1+}'' ($\sim 20\%$). The analysis results for pure oxide and nitrided interface samples are summarized in Table IV.

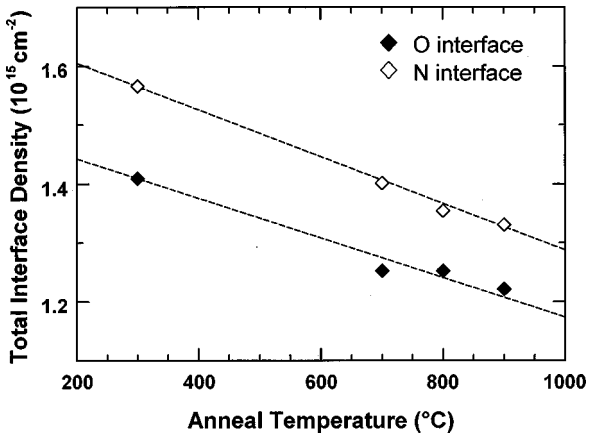

FIG. 8. Average total interface state densities measured from SXPS data for plasma-oxidized Si(111) with and without nitrogen incorporation at the interface. Dashed lines are drawn for illustration only.

TABLE IV. Fitting results summary for interface state densities [1 ML $\sim 7.8\times 10^{14}\,cm^{-2}$ on Si(111)].

Sample	Θ_1 (ML)	Θ_2 (ML)	Θ_3 (ML)	$\Sigma\Theta$ (ML)
SiO_2				
As-grown (300 °C)	0.87	0.59	0.38	1.84
700 °C	0.92	0.26	0.42	1.60
800 °C	0.82	0.23	0.58	1.63
900 °C	0.79	0.30	0.46	1.56
SiO_2/N_2^*				
As-grown (300 °C)	0.91	0.48	0.62	2.01
700 °C	0.80	0.41	0.58	1.79
800 °C	0.70	0.42	0.60	1.73
900 °C	0.70	0.42	0.60	1.72

V. CONCLUSIONS

The Si–SiO_2 interface produced by plasma oxidation has been studied using Si($2p$) core-level photoelectron spectroscopy. The binding energies follow a (~ 1 eV per O ligand) additivity rule as previously reported.[1,2] Deviations from this rule appear as binding energy shifts with SiO_2 film thickness or annealing temperature. In the former, final state effects dominate the shifts, as illustrated by the fact that the magnitude of the shift matches an image-charge correction calculation. Annealing effects are preliminarily assigned as a result of local interface bonding geometry changes, which may affect both initial and final state energies. In particular, Si^{1+} shifts with annealing can be explained by interface Si atoms being drawn into the SiO_2 film as it contracts upon annealing, with an increase in ionic character (Si-to-O charge transfer) of the Si–O bonding. The Si–O–Si bond angle might also change upon annealing, as suggested by Ref. 1.

The reduction of total interface density on Si(111) (in the absence of nitrogen) is due almost entirely to removal of I_2 states (1.84 eV). When nitrogen is present at the interface, it is predominantly the lower (0.96 eV) binding energy state which is removed. Between the 300 °C oxide film growth temperature and an *ex situ* post-oxidation annealing temperature of 900 °C, the total interface density measured by SXPS is reduced by 15%–20%. There is also $\sim 10\%$ more total suboxide in samples with nitrogen incorporated at the interface compared to the pure SiO_2 interface samples. However, the lower binding energy for the film in the nitrided samples may indicate that the nitride layer is effectively an electrical extension of the semiconductor substrate. If so this would be in agreement with electrical measurements which show that the interface state density is lower for nitrided samples compared to the pure SiO_2 interface samples.

Whereas the SXPS data are mostly sensitive to chemical environment, such measurements are not necessarily a good indicator of electrical performance. For example, the measurement of $1.2\times10^{15}\,cm^{-2}$ interface density cannot be expected to be a reliable indicator of the electrically active interface defect density, which is typically three or more orders of magnitude lower.[8] On the other hand, it is conceivable that (for example) some fixed fraction of ''Si^{2+}'' or other nonintrinsic interface states are responsible for charge trapping in the interface and the reduction of this state by annealing helps to reduce this possibility. These questions will be answered in more detail in a forthcoming investigation.

ACKNOWLEDGMENTS

This work is partially supported by the U.S. Army Research Office and the Department of Energy, Office of Basic Energy Sciences. One of the authors (J.W.K.) is indebted to the National Research Council for administering his stipend over the course of this work. The authors are especially grateful to G. K. Wertheim for copies of his fitting codes and for helpful discussions on the fitting procedures. For many other useful discussions and for the preliminary SiO_2 film thickness measurements with ellipsometry, the authors are grateful to D. E. Aspnes and his group in the Physics Department at NCSU.

[1]F. J. Grunthaner and P. J. Grunthaner, Mater. Sci. Rep. **1**, 65 (1986).
[2]F. J. Himpsel, F. R. McFeely, A. Taleb-Ibrahimi, J. A. Yarmoff, and G. Hollinger, Phys. Rev. B **38**, 6084 (1988).
[3]M. M. Banaszak-Holl, S. Lee, and F. R. McFeely, Appl. Phys. Lett. **65**, 1097 (1994).
[4]K. Z. Zhang, M. M. Banaszak-Holl, J. E. Bender, S. Lee, and F. R. McFeely, Phys. Rev. B **54**, 7686 (1996).
[5]F. R. McFeely, K. Z. Zhang, M. M. Banaszak-Holl, S. Lee, and J. E. Bender, J. Vac. Sci. Technol. B **14**, 2824 (1996).
[6]T. Hattori, Appl. Surf. Sci. **130-132**, 156 (1998).
[7]H. Niimi, H. Y. Yang, and G. Lucovsky Proceedings of 1998 Internat. Conference on Characterization and Metrology for ULSI Technology. NIST: Gaithersberg, MD.
[8]C. H. Bjorkman, T. Yasuda, C. E. Shearon, Jr., Y. Ma, G. Lucovsky, U. Emmerichs, C. Meyer, K. Leo, and H. Kurz, J. Vac. Sci. Technol. B **11**, 1521 (1993).
[9]H. Niimi and G. Lucovsky, Surf. Coat. Technol. **98**, 1529 (1998).
[10]H. Niimi, K. Koh, and G. Lucovsky, Electrochem. Soc. Interface **12**, 623 (1996).
[11]G. Lucovsky, H. Niimi, Y. Wu, C. R. Parker, and J. R. Hauser, J. Vac. Sci. Technol. A **16**, 1721 (1998).
[12]G. Lucovsky, J. Vac. Sci. Technol. A **16**, 356 (1998).
[13]J. Schafer, A. P. Young, L. J. Brillson, H. Niimi, and G. Lucovsky, Appl. Phys. Lett. **73**, 791 (1998).
[14]D. G. Sutherland, H. Akatsu, M. Copel, F. J. Himpsel, T. A. Callcott, J. A. Carlisle, D. L. Ederer, J. J. Jia, I. Jiminez, R. Perera, D. K. Shuh, L. J. Terminello, and W. M. Tong, J. Appl. Phys. **78**, 6761 (1995).
[15]P. Thiry, P. A. Bennett, S. D. Kevan, W. A. Royer, E. E. Chaban, J. E. Rowe, and N. V. Smith, Nucl. Instrum. Methods Phys. Res. **222**, 85 (1984).
[16]G. K. Wertheim, J. E. Rowe, D. M. Riffe, and N. V. Smith, AIP Conf. Proc. **215**, 259 (1990).
[17]F. Rochet, C. Poncey, G. Dufour, H. Roulet, C. Guillot, and F. Sirotti, J. Non-Cryst. Solids **216**, 148 (1997).
[18]G. Hollinger, Appl. Surf. Sci. **8**, 318 (1981).
[19]R. Browning, M. A. Sobolewski, and C. R. Helms, in *The Physics and Chemistry of SiO_2 and the Si-SiO_2 Interface*, edited by C. R. Helms and B. E. Deal (Plenum, New York, 1988), pp. 243–250.
[20]A. Pasquarello, M. S. Hybertsen, and R. Car, Phys. Rev. B **53**, 10942 (1996).
[21]The dielectric constant is frequency-dependent. The quasistatic ''DC'' value of ~4 is not applicable in our case, since the time scale of electron emission is on the order of femtoseconds (taking electron kinetic energy and escape depth from our experiments). In this high-frequency range, the dielectric constant takes the ''AC'' value of ~2. See H. Arwin and D. E. Aspnes, J. Vac. Sci. Technol. A **2**, 1316 (1984).
[22]G. K. Wertheim, J. Electron Spectrosc. Relat. Phenom. **60**, 237 (1992).
[23]G. K. Wertheim and S. B. Dicenzo, J. Electron Spectrosc. Relat. Phenom. **37**, 57 (1985).